Materials Chemistry and Physics 140 (2013) 255–259

Contents lists available at SciVerse ScienceDirect

Materials Chemistry and Physics

journal homepage: www.elsevier.com/locate/matchemphys

Structural and thermal evolution studies of $LaSbO_4$ ceramics prepared by solid-state reaction method

Kisla P.F. Siqueira, Raquel M. Borges, Júlia C. Soares, Anderson Dias*

Departamento de Química, Universidade Federal de Ouro Preto, Campus Morro do Cruzeiro, ICEB II, Sala 67, Ouro Preto 35400-000, MG, Brazil

HIGHLIGHTS

- $LaSbO_4$ compounds were produced by solid-state method.
- Structural characterization was conducted by XRD and Raman scattering.
- Polarized Raman spectroscopy in sintered ceramics allowed us a complete modes assignment.
- Luminescence properties revealed a promising phosphor.

ARTICLE INFO

Article history:
Received 13 July 2012
Received in revised form
13 December 2012
Accepted 12 March 2013

Keywords:
A. Electronic materials
B. Raman spectroscopy and scattering
D. Crystal structure
D. Luminescence

ABSTRACT

This work investigates the thermal evolution of $LaSbO_4$ ceramics produced by solid-state method in the temperature range 700–1500 °C, for 6 h. Besides the expected phase transitions, a thermal decomposition at high temperatures to La_3SbO_7 was observed and discussed. The results showed that the phase $LaSbO_4$ can be obtained only below 1450 °C, while temperatures lower than 1100 °C are not able to produce crystalline structures. The samples were submitted to X-ray diffraction and Raman scattering measurements aiming to determine their crystal structures. $LaSbO_4$ materials exhibited monoclinic structures, space group $P2_1/m = C_{2h}^2$(#11), with $Z = 4$. It was verified that all the 36 Raman-active modes predicted by group-theory calculations were observed. Also, the symmetries could be discerned by using polarized Raman scattering, which allow us to assign the *gerade* modes. Luminescence properties of $LaSbO_4$ were investigated and the results showed that this compound exhibits sensitivity of the host lattice to UV excitation. PL spectra excited at 360 nm have a blue emission band maximum at 428 nm, corresponding to the self-activated luminescence center of $LaSbO_4$.

1. Introduction

Compounds of the type ABO_4 (A = rare-earth and B = As, P, V, Nb, Ta, Sb) are very attractive materials because of their chemical and physical properties. The recent papers have been motivated by the fact that these compounds can be used as convenient host materials for fundamental spectroscopic investigations of rare-earth ions, as solid-state laser hosts, and for radioactive waste isolation [1,2], particularly for B = As, P or V. Furthermore, for the compounds with B = Nb and Ta, promising applications involving photo–electronic activity [3–5], ion conductivity [6,7] and luminescence [8–11] have been reported. Recently, Siqueira et al. [12] carried out a detailed investigation on the crystal structure of lanthanide orthoniobates and showed that all samples exhibited monoclinic structure, space group C2/c (#15) and $Z = 4$. For the lanthanide orthotantalates, Siqueira et al. [13] reported that different structures can be obtained as a function of the processing temperature and lanthanide ionic radii. For example, ceramic processing at 1300 °C resulted in three different crystal structures, as follows: monoclinic structure, space group $P2_1/c$ (#14), for RE = La, Ce and Pr; fergusonite M-type, I2/a (#15), for RE = Nd–Tb; and fergusonite M′-type structure, P2/a (#13), for the compounds with smallest ionic radii (RE = Dy–Lu) [13].

For lanthanide orthoantimonates, little information is available from the literature. Gerlach et al. [14] reported the processing of $ASbO_4$ single crystals (A = La, Pr, Nd, Sm, Eu, Gd, Tb, Dy, Lu) through endothermic chemical transport with $TeCl_4$ as transport agent but there are still many divergences about the structure exhibited by these compounds. In view of that, this paper investigates the synthesis, crystal structure and characterization of the $LaSbO_4$ compound, for which only an X-ray powder diffraction was reported

* Corresponding author. Tel.: +55 31 35591716; fax: +55 31 35591707.
E-mail addresses: anderson_dias@iceb.ufop.br, anderson_dias@ig.com.br (A. Dias).

0254-0584/$ – see front matter © 2013 Elsevier B.V. All rights reserved.
http://dx.doi.org/10.1016/j.matchemphys.2013.03.031

[15]. Based on this information and on the similarity with the $LaTaO_4$ compound, previously investigated by our research group [13], we carried out a detailed investigation on the thermal evolution and optimum synthesis conditions to lanthanum orthoantimonates. Also, polarized-Raman scattering and photoluminescence measurements were done aiming to understand the crystal structure, phonon modes and emission properties of the $LaSbO_4$ ceramics. To the best of our knowledge, $LaSbO_4$ compounds obtained by conventional solid-state reaction method were not previously reported by the literature. The goal of this work is to contribute to the understanding of both structural and luminescence properties of this class of materials with promising technological applications.

2. Experimental

$LaSbO_4$ ceramics were synthesized by using La_2O_3 and Sb_2O_5 (>99.9% Sigma–Aldrich) as starting materials through the solid-state reactions. Stoichiometric amounts of the reactants were weighed and mixed with a mortar and pestle. The mixed powders were calcined in the temperature range 700–1500 °C for fixed times of 6 h, with intermediate regrinding. For sintering, cylindrical pucks of about 5 mm height and 12.5 mm diameter were produced by applying a pressure of 150 MPa. The samples were then sintered in a conventional oven at 1500 °C, for 8 h. The crystal structure of the as-synthesized samples were studied by X-ray diffraction (XRD) using a Shimadzu D-6000 diffractometer with graphite monochromator and a nickel filter in the range of 10–60 2θ (15 s step^{-1} of 0.02 2θ), operating with FeKα radiation ($\lambda = 0.1936$ nm), 40 kV and 20 mA (the results were automatically converted to CuKα radiation for data treatment and manipulation). The software MDI Jade 9.0 was employed to calculate the lattice parameters.

Raman spectra of the as-synthesized samples were collected in backscattering configuration using an Horiba/Jobin-Yvon LABRAM-HR spectrometer with the 632.8 nm line of a helium–neon laser (effective power of 6 mW at the sample's surface) as excitation source, diffraction gratings of 600 and 1800 grooves mm^{-1}, Peltier-cooled CCD detector, confocal Olympus microscope (100× objective), and experimental resolution typically 1 cm^{-1} for 10 accumulations of 30 s. Polarized Raman spectra was carried out in the sample sintered at 1500 °C for 8 h. Appropriate interference filter for rejecting laser plasma lines, and edge filter for stray light rejection were used. All resulting spectra were corrected by Bose–Einstein thermal factor [16]. The emission and excitation spectra were acquired under continuous Xe arc lamp (450 W) excitation in a SPEX Triax 550 Fluorolog 3 spectrofluorometer at room temperature. The detection was performed with a Peltier-cooled SPEX Synapse CCD. The emission was collected at 90° from the excitation beam. Filters were placed in the excitation and emission beams, in order to improve the quality of the acquired spectra. For the emission spectra, the entrance and exit slits were adjusted, so as to obtain resolutions of 10–12 and 2 nm, respectively, for the excitation spectra, the resolutions were 2 and 10 nm. All the spectra were corrected, with the software apparatus, for the lamp intensity and photomultiplier sensitivity at the monitored wavelengths.

3. Results and discussion

Fig. 1 presents the XRD results related to the thermal evolution study of the $LaSbO_4$ samples prepared by the solid-state reaction method. This study involved a temperature range of 700–1500 °C with intervals of 200 °C in order to adjust the optimum synthesis conditions and follow the behavior of the thermal treatment on the crystallization phase $LaSbO_4$. As it can be seen, the chemical reaction did not occurred at 700 °C and only the presence of the starting precursors (La_2O_3 and Sb_2O_5) can be observed. Although it is a low

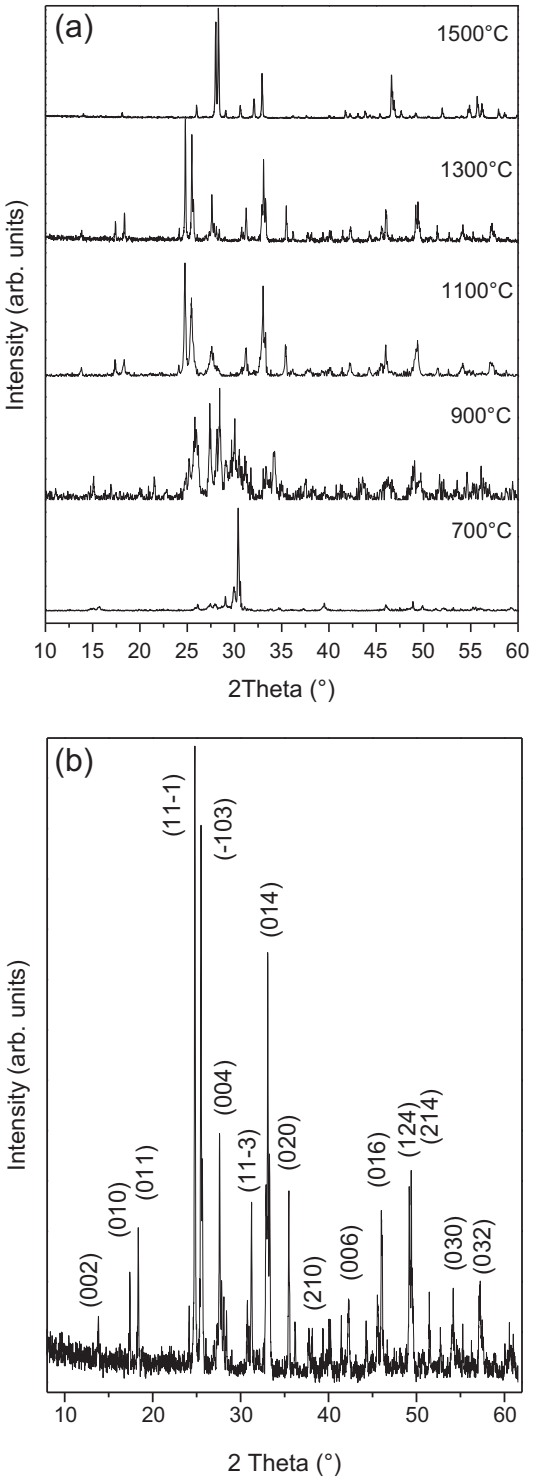

Fig. 1. (a) Thermal evolution for the $LaSbO_4$ compound in the temperature range 700–1500 °C studied by XRD; (b) XRD pattern for the $LaSbO_4$ processed at 1300 °C with the respective crystallographic planes indexed. Note that the $LaSbO_4$ phase was obtained at 1100 and 1300 °C, while the phase La_3SbO_7 was obtained at 1500 °C.

temperature for solid-state reactions in many ceramic systems, we decided to start at 700 °C because of the low melting-point of antimony oxide (Sb_2O_5), which value is 380 °C [17]. Moreover, no information about solid-state reactions for this compound was found in the literature. At 900 °C (Fig. 1a), we can observe the beginning of the chemical reaction, but no formation of $LaSbO_4$. Only above 1100 °C it was possible to obtain the $LaSbO_4$ in a single

phase form, without contaminants or secondary phases. Ceramics processed at 1300 °C exhibit a higher degree of crystallinity than the samples synthesized at 1100 °C, and could be indexed with ICDD (International Committee for Diffraction Data) card number #36-0950. Fig. 1b shows the respective crystallographic planes indexed for this sample. The $LaSbO_4$ compound exhibited a monoclinic structure with space group $P2_1/m = C_{2h}^2$ (#11), and four units per unit cell. The calculated lattice parameters are: $a = 5.115$ Å; $b = 5.055$ Å; $c = 12.990$ Å and $\beta = 96.28°$. The crystal structure of $LaSbO_4$ contains chains of [SbO_6] octahedra connected via common edges [18].

In spite that we have already achieved a crystalline phase, our study was beyond and additional experiments were conducted at higher temperatures in order to observe a possible phase transition, as detected by Gerlach et al. [14] in $PrSbO_4$ ceramics. In this case, the authors observed that the samples crystallized in two different structures (α-$PrSbO_4$ and β-$PrSbO_4$) as a function of the processing temperature. Based on these results, we carried out experimental synthesis also at 1500 °C. Unlike the expected phase transition at 1500 °C, the resulting sample exhibited a thermal decomposition toward La_3SbO_7 (Fig. 1a), indexed by the ICDD card #23-1138, which refers to an orthorhombic structure. Therefore, experimental tests at lower temperatures were carried out between 1300 °C and 1500 °C aiming to investigate and determine the temperature which the $LaSbO_4$ ceramic decomposes to La_3SbO_7. The results showed that the $LaSbO_4$ phase can be produced at temperatures below 1450 °C using a fixed time of 6 h. It was observed that temperatures equal or higher than 1450 °C can lead to a preferential crystallization of La_3SbO_7, despite all stoichiometric calculations made for the production of $LaSbO_4$.

According to the literature, there are many reports on the synthesis and crystal properties of La_3SbO_7 materials [19,20], while for the $LaSbO_4$ ceramic there are practically no papers. Our results suggest that at high temperatures (1450 °C and above) the loss of Sb_2O_5 by volatilization could occur because to its low melting-point, as already discussed, which causes the lack of this unit (Sb_2O_5) in the original structure and avoid the formation of the stoichiometric phase $LaSbO_4$. Similar behavior was noted by Ok et al. [21] in their work about the new compounds $LaSb_5O_{12}$ and $LaSb_3O_9$. The authors noted that the phase $LaSb_3O_9$ is stable only below 1100 °C. When this sample is heated at higher temperatures, it was observed the decomposition to $LaSbO_4$ according to the Eq. (1) [21]. Following this reasoning, if we "subtract" one Sb_2O_5 unit from the stoichiometric $LaSbO_4$, we can get La_3SbO_7, according to the Eq. (2):

$$LaSb_3O_9 - Sb_2O_5 \rightarrow LaSbO_4 \quad (1)$$

$$3LaSbO_4 - Sb_2O_5 \rightarrow La_3SbO_7 \quad (2)$$

In this case, we believe that the processing at high temperatures can result in the shortage of antimony (V) oxide because of its low thermal stability. Thermal studies in compounds of the type $NdBO_4$ (B = P, As and Sb) showed that among all these compositions the $NdSbO_4$ presented the lowest thermal stability (Sb < As < P) [14].

Now, the results obtained from Raman scattering measurements in $LaSbO_4$ samples synthesized in optimized conditions will be presented. Group-theory calculations were made based on those previously reported for the $LaTaO_4$ compounds [13], since there is no vibrational spectroscopic information concerning $LaSbO_4$ materials in the literature. For this system, lanthanum, antimony and four oxygen atoms should occupy the 4*f* sites of symmetry C_1. Due to these occupation sites, the Raman-active modes of this system can be decomposed according to the irreducible representation (i.r.) of the C_1 point-group, as shown in Table 1. Then, using the site-group method of Rousseau et al. [22] we can obtain the following distribution of the degrees of freedom at Brillouin-zone center in terms of the i.r. of the C_{2h}^2 point group:

Table 1
Factor-group analysis for the $LaSbO_4$ compound at room temperature.

Ion	Wyckoff sites	Symmetry	Irreducible representations
La	4*f*	C_1	$3A_g + 3A_u + 3B_g + 3B_u$
Sb	4*f*	C_1	$3A_g + 3A_u + 3B_g + 3B_u$
O(1)	4*f*	C_1	$3A_g + 3A_u + 3B_g + 3B_u$
O(2)	4*f*	C_1	$3A_g + 3A_u + 3B_g + 3B_u$
O(3)	4*f*	C_1	$3A_g + 3A_u + 3B_g + 3B_u$
O(4)	4*f*	C_1	$3A_g + 3A_u + 3B_g + 3B_u$
		$\Gamma_{ACOUSTIC}$	$A_u + 2B_u$
		Γ_{RAMAN}	$18A_g + 18B_g$

$$\Gamma_{TOTAL} = 18A_g + 18B_g + 18A_u + 18B_u \quad (3)$$

Thus, we would expect 36 *gerade* Raman modes ($18A_g + 18B_g$) for the $LaSbO_4$ system. Raman spectra were obtained at room temperature for $LaSbO_4$ samples synthesized at 1300 °C. Because of the high number of active modes, a careful analysis was carried out by fitting the Raman experimental data with Lorentzian curves as it can be seen in Fig. 2 (green lines), which was divided up into three different wavenumber regions with numbered bands for better visualization. The experimental data are in closed squares, whereas the fitting curves are presented by red lines. The results showed that 36 Raman modes can be fitted, in perfect agreement with the theoretical predictions.

Following, the results obtained from polarized Raman spectroscopy will be presented. For this study, a ceramic was sintered at 1500 °C for 8 h. These processing conditions were employed because the goal was to obtain ceramics with large grains in order

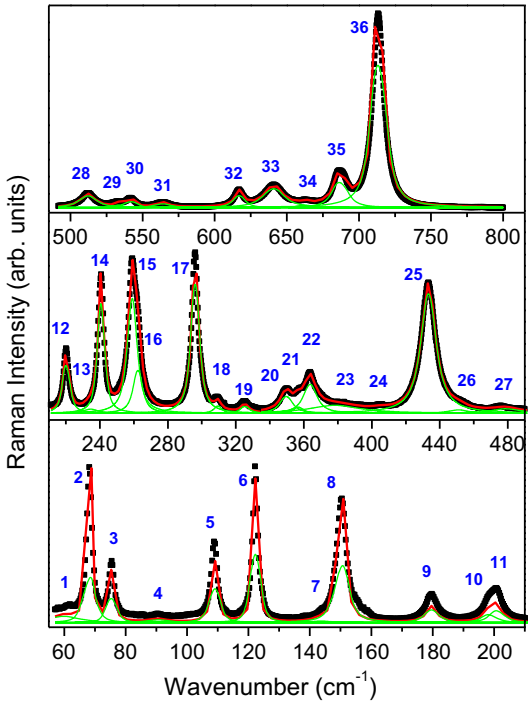

Fig. 2. Micro-Raman spectra for the $LaSbO_4$ sample in the spectral region 50–800 cm^{-1}. Experimental data are in closed squares, whereas the fitting curves are represented by red lines. Green lines represent the phonon modes adjusted by Lorentzian curves. The Raman-active modes were numbered for better visualization. (For interpretation of the references to color in this figure legend, the reader is referred to the web version of this article.)

to get suitable polarized Raman measurement. For the sintering process, it was necessary to involve the compacted ceramics into the loose powders ($LaSbO_4$) to avoid the antimony loss by volatilization and consequently the decomposition to La_3SbO_7, already discussed. However, the phase decomposition along the surface of the sintered ceramics was inevitable. Crystalline, single phase $LaSbO_4$ materials were obtained only in the internal part of the sintered pucks. It was not detected the existence of polymorphs, since the phase $LaSbO_4$ formed at 1500 °C was identical to the previously produced by calcining at 1300 °C. Furthermore, the grain growth allowed the analysis of the sample by polarized Raman spectroscopy.

It is well-known that the inelastic scattered light intensities due to the Raman effect are proportional to the square of the elements of the polarizability tensor (second-order tensor). Then, the base functions of the i.r. that contain the Raman-active modes have a quadratic form, i.e., they transform like the product of the Cartesian coordinates. For single crystals, we take benefit of the crystal symmetry to assign the lattice vibrations to the different i.r. [16,22]. However, in the case of the ceramics, although the group-theory predictions remain valid, the symmetry of the modes is generally mixed due to the random orientation of the crystalline grains. In this work, we have used a confocal microscope with an objective of magnification of 100×, which allows the selection of an observation region as small as 2 μm on the sample surface or even inside the sample. Nevertheless, we do not know anything about the crystallographic axes of these grains, which have also random orientation throughout the sample. By measuring the micro-Raman spectra of $LaSbO_4$ sintered sample with cross-polarized light (Fig. 3), we observed that for some grains the spectra of parallel (red line) and crossed light (blue line) become different. We can observed the relative strengthening of the A_g modes in the parallel configuration accompanied by the relative weakening of the B_g modes, which are favored by crossed light configuration. Therefore, we could assign all the 36 Raman-active *gerade* modes as belonging to the A_g and B_g symmetries, as presented in Table 2.

We will now discuss the luminescence behavior of our $LaSbO_4$ samples. Fig. 4 shows the excitation spectrum (Fig. 4a) and emission spectrum (Fig. 4b) obtained for the $LaSbO_4$ ceramics. The optical transition of niobate and tantalate groups have been ascribed to a charge-transfer process [23,24]. For the antimonate groups, the same situation can be considered. $LaSbO_4$ is an undoped phosphor that under different exciting radiations shows UV-blue emission due to the charge transfer transition into SbO_4 group. We can consider that the conduction band is composed by Sb^{5+} 4*d* orbitals and the valence band by O^{2-} 2*p* orbitals, similarly as found for $LaNbO_4$ through electronic structure calculations [25]. Photoluminescence (PL) profiles for $LaSbO_4$ powders (Fig. 4) suggest a mechanism by multilevel process, in which the relaxation of the system occurs by means of several paths, involving the participation of several energy states within the band gap of the material [26]. We believe that the multilevel processes are occurring in our samples because the spectra presented in this work are very similar with those obtained for other tungstate samples [26]. Furthermore, the spectra were deconvoluted using Lorentzian curves and the PL profiles were better adjusted by four peaks, as it can be seen in Fig. 4. The maximum excitation peak is localized at 376 nm, but the other three peaks can be visualized at around 330, 357 and 398 nm. All these peaks are associated with the direct excitation of $LaSbO_4$ host itself via charge transfer transition between Sb and O. On the other hand, the emission spectrum shows the peaks at around 403, 428, 456 and 489 nm, being the more intense peak the located at 428 nm. Hsiao et al. [25] also found more than one peak for both excitation and emission spectra in $LaNbO_4$ samples. In this case, the authors attributed these results to presence of absorbing groups NbO_4 and NbO_6. The excitation and emission spectra of the lanthanum antimonates are red shifted if compared to lanthanum niobates ($LaNbO_4$: excitation at 260 nm and emission at 408 nm [25]). This behavior is due to the higher 5th ionization potential (I_5 = 50.5 eV, for Nb, and 56.0 eV, for Sb). Blasse and Bril [23]

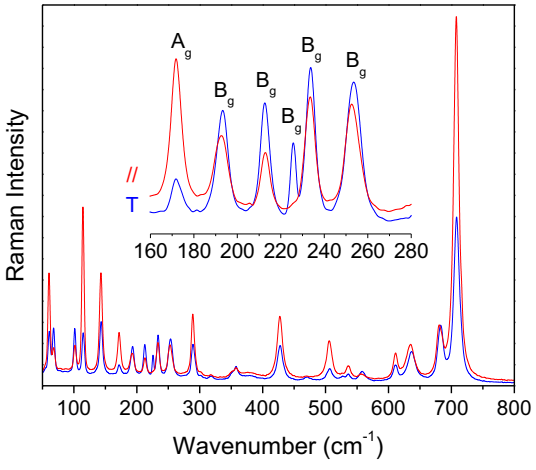

Fig. 3. Polarized Raman scattering for the sintered $LaSbO_4$ ceramics. Parallel (//) and cross-polarized (T) configurations are indicated in red and blue lines, respectively. Inset: the relative strengthening of the A_g modes in the parallel configuration accompanied by the relative weakening of the B_g modes, which are favored by crossed light configuration. (For interpretation of the references to color in this figure legend, the reader is referred to the web version of this article.)

Table 2
Phonon wavenumbers (cm^{-1}) and assignment of the *gerade* modes, determined from the adjustment of the Raman experimental data by Lorentzian lines for the $LaSbO_4$.

Band	Assignment	Wavenumber
1	B_g	60
2	A_g	68
3	B_g	76
4	A_g	91
5	B_g	109
6	A_g	122
7	B_g	144
8	A_g	150
9	A_g	180
10	B_g	198
11	B_g	201
12	B_g	220
13	B_g	235
14	B_g	241
15	B_g	259
16	B_g	262
17	A_g	296
18	B_g	309
19	B_g	325
20	A_g	433
21	A_g	479
22	B_g	451
23	A_g	405
24	A_g	378
25	A_g	364
26	A_g	357
27	B_g	350
28	A_g	512
29	B_g	532
30	A_g	542
31	B_g	564
32	A_g	617
33	A_g	641
34	A_g	663
35	B_g	687
36	A_g	714

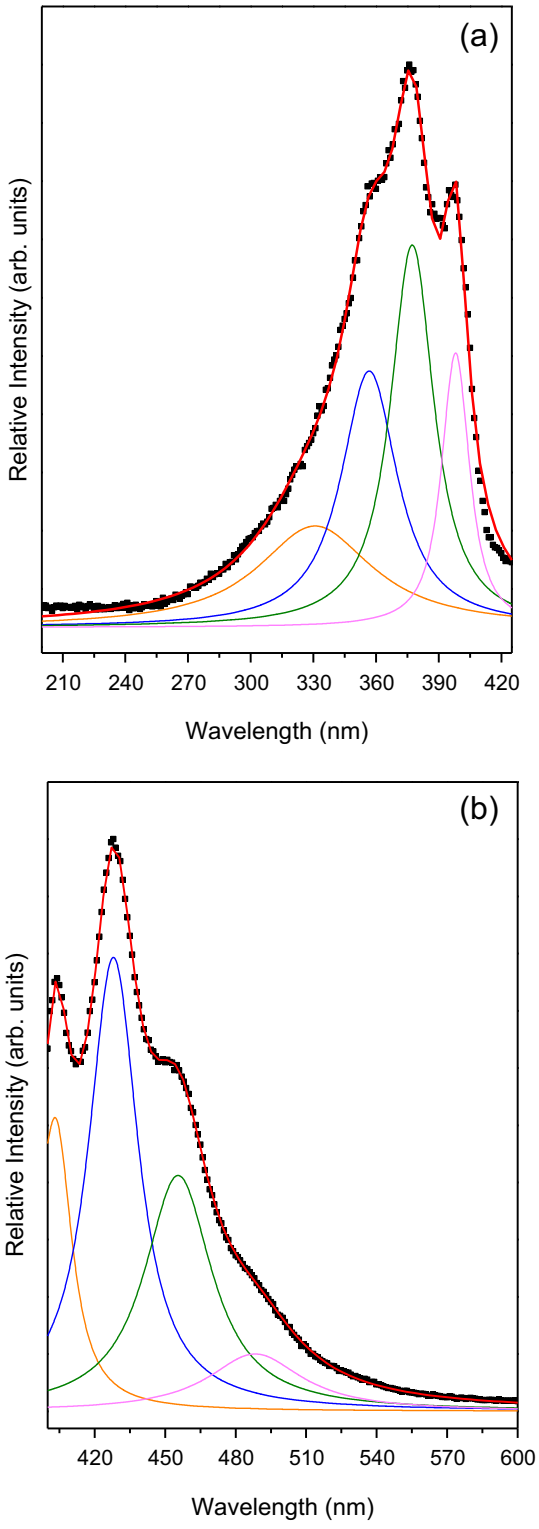

Fig. 4. (a) Excitation ($\lambda_{em} = 428$ nm) and (b) emission ($\lambda_{ex} = 360$ nm) spectra at room temperature for the phosphor $LaSbO_4$. Note that the spectra were deconvoluted using Lorentzian curves and they were necessary to use four peaks (represented by different colors) to better adjusted the PL spectra. The experimental data are in closed squares (black), whereas the fitting curves are represented by red lines. (For interpretation of the references to color in this figure legend, the reader is referred to the web version of this article.)

showed that the lower 5th ionization potential of the metal resulted in a greater energy required for the charge transfer transitions of the BO_4 groups. As a consequence, the excitation and emission spectra of the niobates are shifted to higher energies relative to the antimonates. Thus, our PL results are in totally agreement with theory prediction.

4. Conclusions

$LaSbO_4$ ceramics were synthesized by solid-state reactions in optimized temperatures, for fixed times of 6 h. The thermal evolution for this material showed that only in the temperature range of 1100–1450 °C the $LaSbO_4$ ceramics can be formed. For temperatures above 1450 °C, the main phase decomposes to La_3SbO_7, probably due to volatilization of Sb_2O_5. XRD results showed that the orthoceramic was obtained without impurities, crystallizing in the monoclinic structure with space group $P2_1/m = C_{2h}^2(\#11)$ and $Z = 4$. Raman spectroscopy was employed to determine all the 36 phonon-modes predicted by group-theory calculations, which can be discerned by using polarized scattering. The optical properties of $LaSbO_4$ ceramics were investigated by photoluminescence measurements. The PL spectrum excited at 360 nm showed a blue emission band maximum of 428 nm, corresponding to the self-activated luminescence center of $LaSbO_4$.

Acknowledgments

The authors acknowledge the financial support from CNPq, FINEP and FAPEMIG. This work is a collaborative research project with members of the Rede Mineira de Química (RQ-MG), who are supported by FAPEMIG. Special thanks to Prof. Dr. Osvaldo Antonio Serra and Paulo C. de Sousa Filho for their hospitality during PL measurements.

References

[1] W.J. Weber, R.C. Ewing, C.R.A. Catlow, T.D. dela Rubia, L.W. Hobbs, C. Kinoshita, H. Matzke, A.T. Motta, M. Nastasi, E.K.H. Salje, E.R. Vance, S.J. Zinkle, J. Mater. Res. 13 (1998) 1434–1484.
[2] A. Brenier, G. Jia, C. Tu, J. Phys. Condens. Matter 16 (2004) 9103–9108.
[3] K. Shimizu, S. Itoh, T. Hatamachi, T. Kodama, M. Sato, K. Toda, Chem. Mater. 17 (2005) 5161–5166.
[4] F.E. Osterloh, Chem. Mater. 20 (2008) 35–54.
[5] R. Abe, M. Higashi, Z.G. Zou, K. Sayama, Y. Abe, H. Arakawa, J. Phys. Chem. B 108 (2004) 811–814.
[6] R. Haugsrud, T. Norby, Nat. Mater. 5 (2006) 193–196.
[7] T. Mokkelbost, Ø. Andersen, R.A. Strom, K. Wiik, T. Grande, M. Einarsrud, J. Am. Ceram. Soc. 90 (2007) 3395–3400.
[8] B. Li, Z. Gu, J. Lin, M.Z. Su, Mater. Res. Bull. 35 (2000) 1921–1931.
[9] T. Pang, W. Cao, Y. Fu, X. Luo, Mater. Lett. 62 (2008) 2500–2502.
[10] B. Liu, K. Han, X. Liu, M. Gu, S. Huang, C. Ni, Z. Qi, G. Zhang, Solid State Commun. 144 (2007) 484–487.
[11] X. Xiao, B. Yan, J. Non-Cryst. Solids 351 (2005) 3634–3639.
[12] K.P.F. Siqueira, R.L. Moreira, A. Dias, Chem. Mater. 22 (2010) 2668–2674.
[13] K.P.F. Siqueira, G.B. Carvalho, A. Dias, Dalton Trans. 40 (2011) 9454–9460.
[14] S. Gerlach, R.C. Gil, E. Milke, M. Schmidt, Z. Anorg. Allg. Chem. 633 (2007) 83–92.
[15] M.B. Varfolomeev, T.A. Toporenskaya, B.A. Narnov, Russ. J. Inorg. Chem. (Engl. Transl.) 26 (1981) 171–173.
[16] W. Hayes, R. Loudon, Scattering of Light by Crystals, Wiley, New York, 1978.
[17] P. Patnaik, Handbook of Inorganic Chemicals, McGraw-Hill, 2002.
[18] C. Hirschle, J. Rosstaucher, C. Rohr, Acta Crystallogr. Sect. C C57 (2001) 1239–1241.
[19] M. Wakeshima, Y. Hinatsu, J. Solid State Chem. 183 (2010) 2681–2688.
[20] Y. Hinatsu, H. Ebisawa, Y. Doi, J. Solid State Chem. 182 (2009) 1694–1699.
[21] K.M. Ok, A. Guittens, L. Zhang, P.S. Halasyamani, J. Mater. Chem. 14 (2004) 116–120.
[22] D.L. Rousseau, R.P. Bauman, S.P.S. Porto, J. Raman Spectrosc. 10 (1981) 253–290.
[23] G. Blasse, A. Bril, J. Lumin. 3 (1970) 109–131.
[24] E.C. Karsu, E.J. Popovici, A. Ege, M. Morar, E. Indrea, T. Karali, N. Can, J. Lumin. 131 (2011) 1052–1057.
[25] Y.J. Hsiao, T.H. Fang, Y.S. Chang, Y.H. Chang, C.H. Liu, L.W. Ji, W.Y. Jywe, J. Lumin. 126 (2007) 866–870.
[26] J.C. Sczancoski, L.S. Cavalcante, M.R. Joya, J.W.M. Espinosa, P.S. Pizani, J.A. Varela, E. Longo, J. Colloid Interface Sci. 330 (2009) 227–236.